Negative magnetoresistence in Dirac Semimetals from Keldysh technique

Ruslan Abramchuk[1] M.A.Zubkov[1]

Physics Department, Ariel University, Ariel 40700, Israel[1]

On-line talk at the Chirality2024 conference
July 23, 2024

CKT and CME

The renowned theory suggests [Fukushima, Kharzeev, Warringa Phys.Rev.D78 074033 (2008), Li and Kharzeev et al. Nature Physics 12, 550-554 (2016)], that in a system that hosts massless Dirac fermions, chiral anomaly pumps up chiral density

$$\rho_5 = \rho_R - \rho_L = N_f \frac{\vec{E} \cdot \vec{H}}{4\pi^2} \tau_5, \tag{1}$$

CKT and CME

The renowned theory suggests [Fukushima, Kharzeev, Warringa Phys.Rev.D78 074033 (2008), Li and Kharzeev et al. Nature Physics 12, 550-554 (2016)], that in a system that hosts massless Dirac fermions, chiral anomaly pumps up chiral density

$$\rho_5 = \rho_R - \rho_L = N_f \frac{\vec{E} \cdot \vec{H}}{4\pi^2} \tau_5, \tag{1}$$

which yields chiral the chemical potential

$$\rho_5 \approx \frac{\mu_5}{3v_F^3}\left(T^2 + \mu^2/\pi\right), \tag{2}$$

CKT and CME

The renowned theory suggests [Fukushima, Kharzeev, Warringa Phys.Rev.D78 074033 (2008), Li and Kharzeev et al. Nature Physics 12, 550-554 (2016)], that in a system that hosts massless Dirac fermions, chiral anomaly pumps up chiral density

$$\rho_5 = \rho_R - \rho_L = N_f \frac{\vec{E} \cdot \vec{H}}{4\pi^2} \; \tau_5, \tag{1}$$

which yields chiral the chemical potential

$$\rho_5 \approx \frac{\mu_5}{3v_F^3}\left(T^2 + \mu^2/\pi\right), \tag{2}$$

which via CME

$$\vec{j} = \frac{1}{2\pi^2}\mu_5 \vec{H} \tag{3}$$

CKT and CME

The renowned theory suggests [Fukushima, Kharzeev, Warringa Phys.Rev.D78 074033 (2008), Li and Kharzeev et al. Nature Physics 12, 550-554 (2016)], that in a system that hosts massless Dirac fermions, chiral anomaly pumps up chiral density

$$\rho_5 = \rho_R - \rho_L = N_f \frac{\vec{E} \cdot \vec{H}}{4\pi^2} \tau_5, \tag{1}$$

which yields chiral the chemical potential

$$\rho_5 \approx \frac{\mu_5}{3v_F^3}\left(T^2 + \mu^2/\pi\right), \tag{2}$$

which via CME

$$\vec{j} = \frac{1}{2\pi^2}\mu_5 \vec{H} \tag{3}$$

yields (actually, observed!) magnetoconductivity

$$\sigma^{ij}_{CME} = \frac{3}{2} N_f \frac{H^i H^j}{4\pi^2} \frac{v_F^3}{\pi^2 T^2 + \mu^2} \tau_5 \tag{4}$$

The gap in real materials

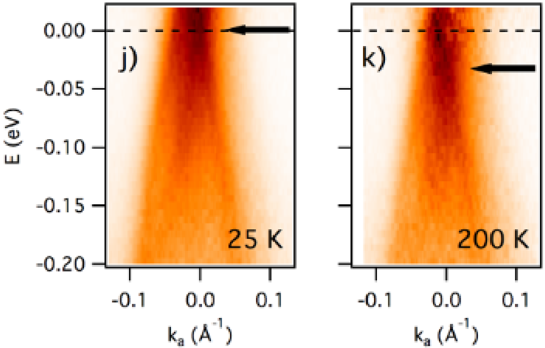

Figure: ARPES for $ZrTe_5$ [Li and Kharzeev et al. Nature Physics 12, 550-554 (2016)]

The gap in real materials

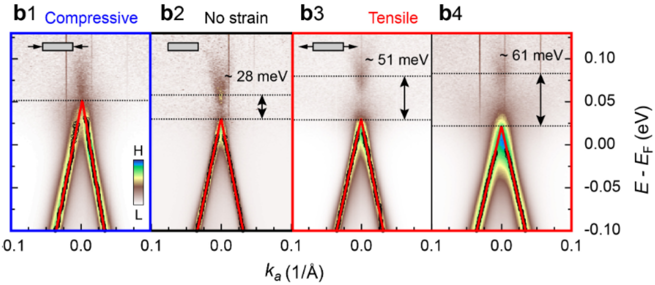

Figure: ARPES for $ZrTe_5$ [Zhang et al. Nature Communications 12, 406 (2021)]

The gap in real materials

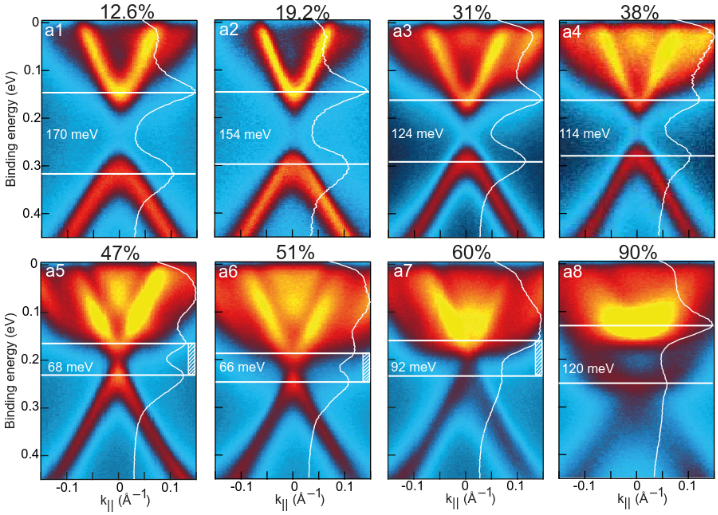

Figure: ARPES for $Mn_{1-x}Ge_xBi_2Te_4$ [Shikin et al. arXiv:2406.15065]

An idea for the chirality relaxation mechanism

Though the gap $2m$ can be negligible in comparison to the chemical potential μ (the non-ideal Fermi-point is deep in the Fermi sphere), the gap indicates the chiral symmetry breaking, which, with some energy dissipation mechanism, can constitute a chirality relaxation mechanism

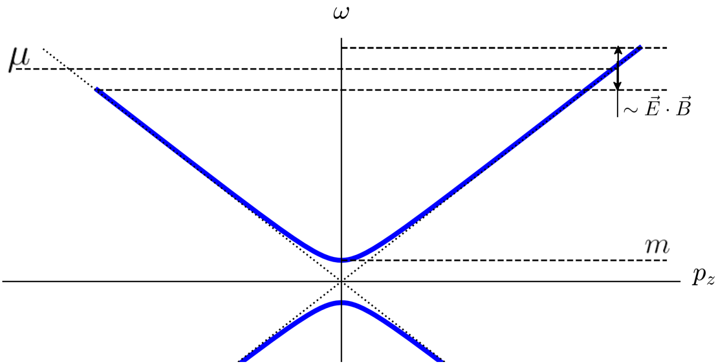

Figure: A sketch of the non-equilibrium stationary population density that accompanies the magnetoconductivity

Non-equilibrium Diagram Technique for relativistic fermions

For Dirac fermions (let $v_F, e \to 1$, etc.)

$$\mathscr{L}_0 = \bar{\psi}(\gamma^\mu(\partial_\mu - ieA_\mu) - m)\psi, \tag{5}$$

Non-equilibrium Diagram Technique for relativistic fermions

For Dirac fermions (let $v_F, e \to 1$, etc.)

$$\mathscr{L}_0 = \bar{\psi}(\gamma^\mu(\partial_\mu - ieA_\mu) - m)\psi, \qquad (5)$$

Keldysh-Green's functions satisfy

$$\hat{Q} = \begin{pmatrix} Q^R & Q^< \\ 0 & Q^A \end{pmatrix}, \quad \hat{G} = \begin{pmatrix} G^R & G^< \\ 0 & G^A \end{pmatrix} \equiv \hat{Q}^{-1}, \qquad (6)$$

Non-equilibrium Diagram Technique for relativistic fermions

For Dirac fermions (let $v_F, e \to 1$, etc.)

$$\mathscr{L}_0 = \bar{\psi}(\gamma^\mu(\partial_\mu - ieA_\mu) - m)\psi, \tag{5}$$

Keldysh-Green's functions satisfy

$$\hat{Q} = \begin{pmatrix} Q^R & Q^< \\ 0 & Q^A \end{pmatrix}, \quad \hat{G} = \begin{pmatrix} G^R & G^< \\ 0 & G^A \end{pmatrix} \equiv \hat{Q}^{-1}, \tag{6}$$

$$Q^{R(A)} = p_0 \pm i\epsilon - (\alpha_i p^i + \gamma_0 m), \; Q^< = -2i\epsilon n(p_0), \tag{7}$$

Non-equilibrium Diagram Technique for relativistic fermions

For Dirac fermions (let $v_F, e \to 1$, etc.)

$$\mathscr{L}_0 = \bar{\psi}(\gamma^\mu(\partial_\mu - ieA_\mu) - m)\psi, \tag{5}$$

Keldysh-Green's functions satisfy

$$\hat{Q} = \begin{pmatrix} Q^R & Q^< \\ 0 & Q^A \end{pmatrix}, \quad \hat{G} = \begin{pmatrix} G^R & G^< \\ 0 & G^A \end{pmatrix} \equiv \hat{Q}^{-1}, \tag{6}$$

$$Q^{R(A)} = p_0 \pm i\epsilon - (\alpha_i p^i + \gamma_0 m), \;\; Q^< = -2i\epsilon n(p_0), \tag{7}$$

than

$$G^{R(A)} = Q^{R(A)-1} = (p_0 \pm i\epsilon - (\alpha_i p^i + \gamma_0 m))^{-1}, \tag{8}$$

Non-equilibrium Diagram Technique for relativistic fermions

For Dirac fermions (let $v_F, e \to 1$, etc.)

$$\mathscr{L}_0 = \bar{\psi}(\gamma^\mu(\partial_\mu - ieA_\mu) - m)\psi, \tag{5}$$

Keldysh-Green‘s functions satisfy

$$\hat{Q} = \begin{pmatrix} Q^R & Q^< \\ 0 & Q^A \end{pmatrix}, \quad \hat{G} = \begin{pmatrix} G^R & G^< \\ 0 & G^A \end{pmatrix} \equiv \hat{Q}^{-1}, \tag{6}$$

$$Q^{R(A)} = p_0 \pm i\epsilon - (\alpha_i p^i + \gamma_0 m), \;\; Q^< = -2i\epsilon n(p_0), \tag{7}$$

than

$$G^{R(A)} = Q^{R(A)-1} = (p_0 \pm i\epsilon - (\alpha_i p^i + \gamma_0 m))^{-1}, \tag{8}$$

$$G^< = -G^R Q^< G^A = (G^A - G^R) n(p_0) \tag{9}$$

Non-equilibrium Diagram Technique for electron-phonon interaction

$$\hat{H}_{\text{e-ph}} = \int d^3x \, \frac{w\hat{\rho}'}{\rho_0} \, \hat{\psi}^\dagger \hat{\psi}, \tag{10}$$

where $w, \; \rho_0$ — crystal's elastic properties.

Non-equilibrium Diagram Technique for electron-phonon interaction

$$\hat{H}_{\text{e-ph}} = \int d^3x \, \frac{w\hat{\rho}'}{\rho_0} \, \hat{\psi}^\dagger \hat{\psi}, \tag{10}$$

where w, ρ_0 — crystal's elastic properties.

$$N_k = (e^{\beta uk} - 1)^{-1}, \text{ where } u = \frac{s}{v_F} \ll 1 \tag{11}$$

is speed of sound for the acoustic phonons, so the effective temperature for the phonons $T_{eff} = \frac{T}{u} \gg T$ than the electrons temperature.

Non-equilibrium Diagram Technique for electron-phonon interaction

$$\hat{H}_{\text{e-ph}} = \int d^3x \, \frac{w\hat{\rho}'}{\rho_0} \, \hat{\psi}^\dagger \hat{\psi}, \tag{10}$$

where w, ρ_0 — crystal's elastic properties.

$$N_{\mathrm{k}} = (e^{\beta uk} - 1)^{-1}, \text{ where } u = \frac{s}{v_F} \ll 1 \tag{11}$$

is speed of sound for the acoustic phonons, so the effective temperature for the phonons $T_{eff} = \frac{T}{u} \gg T$ than the electrons temperature. And the Keldysh-Green's functions

$$D^R = D^{--} - D^{-+} = \frac{\rho_0 k^2}{(\omega + i\epsilon)^2 - u^2 k^2}, \tag{12}$$

$$D^< = D^{-+} = -i\pi \frac{\rho_0 k}{u} (N_{\mathrm{k}} \delta(\omega - uk) + (1 + N_{-\mathrm{k}})\delta(\omega + uk))$$

Magnetoconductivity from NDT

$j_i^{(2)} =$

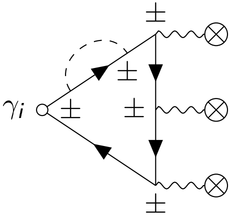

$+$ dozens of diagrams

Magnetoconductivity from NDT

$j_i^{(2)} = \quad \gamma_i$

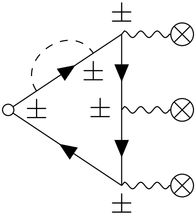

$+$ dozens of diagrams

$$\sim E_j H^j H_i ,$$

Magnetoconductivity from NDT

$j_i^{(2)} = \quad \gamma_i$ 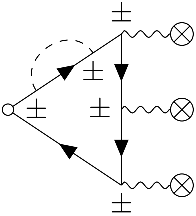

$+$ dozens of diagrams

$\approx \quad \gamma_i$ 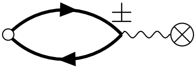

$E_j \quad \sim E_j H^j H_i,$

Magnetoconductivity from NDT

$j_i^{(2)} =$ 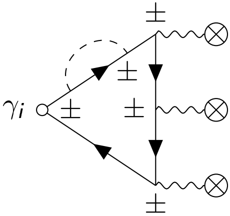

$+$ dozens of diagrams

$\approx$ 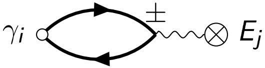

$\sim E_j H^j H_i,$


$=$ 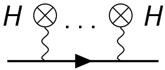

,

Magnetoconductivity from NDT

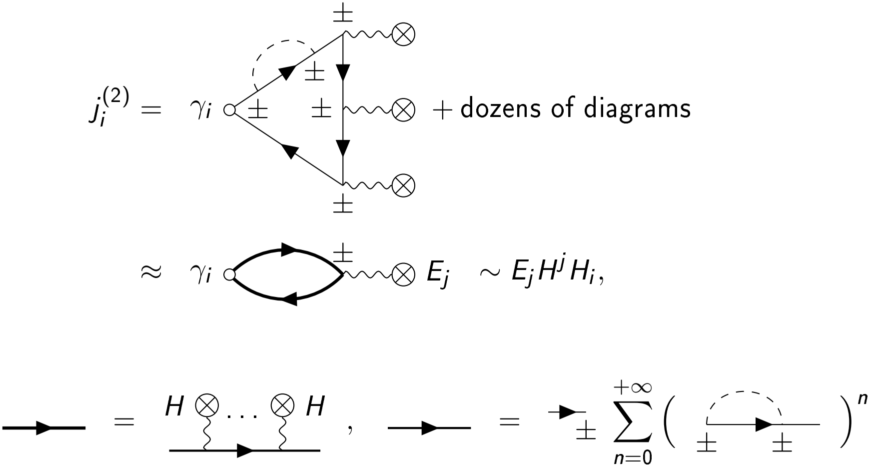

Effective diagram technique. Constant width

$$\hat{G}_{(1)} = $$  $$_{\pm} \sum_{n=0}^{+\infty} \Big($$  $$_{\pm \qquad \pm} \Big)^n = (\hat{Q} - \hat{\Sigma})^{-1}, \qquad (13)$$

$$G^R = (p_0 \pm i\epsilon - \mathscr{H})^{-1}, \qquad (14)$$

Effective diagram technique. Constant width

$\hat{G}_{(1)} =$

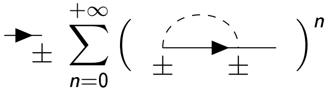

$$= (\hat{Q} - \hat{\Sigma})^{-1}, \tag{13}$$

$$G^R = (p_0 \pm i\epsilon - \mathscr{H})^{-1}, \tag{14}$$

Electron coupling to the thermal bath of acoustic phonons provides an energy dissipation mechanism.

Effective diagram technique. Constant width

$$\hat{G}_{(1)} =$$ 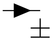 $$\sum_{n=0}^{+\infty} \Big($$ 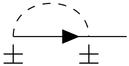 $$\Big)^n = (\hat{Q} - \hat{\Sigma})^{-1}, \quad (13)$$

$$G^R = (p_0 \pm i\epsilon - \mathscr{H})^{-1}, \quad (14)$$

Electron coupling to the thermal bath of acoustic phonons provides an energy dissipation mechanism. We estimate the energy dissipation rate at the Fermi surface

$$\epsilon \approx -\mathrm{Im}\frac{1}{4}\mathrm{tr}\ \Sigma_R(p_0 \sim \mu, |\mathrm{p}| \sim \mu) \quad (15)$$

$$= -\ \mathrm{Im}\ \frac{1}{4}\mathrm{tr}\ \left[ig^2 G^R D^<\right]\Big|_{(p_0\sim\mu,|\mathrm{p}|\sim\mu)} \quad (16)$$

$$\ldots \approx \frac{1}{2\pi}\frac{w^2}{\rho_0}\frac{\mu^2 T}{u^2}, \qquad \frac{u\mu}{T} \ll 1. \quad (17)$$

Effective diagram technique. Weak magnetic field

$$ \tag{18} $$

$$G_H^{R(A)}\gamma_0 = \tag{19}$$

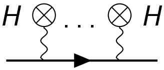

$$ \tag{21} $$

Effective diagram technique. Weak magnetic field

$$\not{D}^2 = D^2 + \frac{1}{2}\sigma_{\mu\nu} i\mathcal{F}^{\mu\nu} \tag{18}$$

$$G_H^{R(A)}\gamma_0 = \tag{19}$$

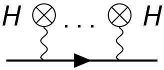

(21)

Effective diagram technique. Weak magnetic field

$$\not{D}^2 = D^2 + \frac{1}{2}\sigma_{\mu\nu} i\mathcal{F}^{\mu\nu} \tag{18}$$

$$G_H^{R(A)}\gamma_0 = \tag{19}$$

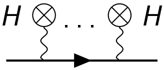

$$= (\not{D}_\pm + m)(D_\pm^2 - m^2 - \Sigma H)^{-1} \tag{20}$$

$$= (\not{D}_\pm + m)\Big((D_\pm^2 - m^2)\Big(1 - \frac{\Sigma H}{D_\pm^2 - m^2}\Big)\Big)^{-1}$$

$$\approx G^{R(A)}\gamma_0\Big(1 + \frac{\Sigma H}{D_\pm^2 - m^2} + \frac{\frac{1}{4}H^2}{(D_\pm^2 - m^2)^2}\Big), \tag{21}$$

where $D_\pm^\mu = \partial^\mu - ie\mathcal{A}_H^\mu \pm \delta^{\mu 0}\epsilon$.

Effective diagram technique. Weak magnetic field

$$\not{D}^2 = D^2 + \frac{1}{2}\sigma_{\mu\nu} i\mathcal{F}^{\mu\nu} \to -p^2 + \Sigma H, \tag{18}$$

$$G_H^{R(A)}\gamma_0 = \tag{19}$$

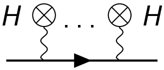

$$= (\not{D}_\pm + m)(D_\pm^2 - m^2 - \Sigma H)^{-1} \tag{20}$$

$$= (\not{D}_\pm + m)\Big((D_\pm^2 - m^2)\Big(1 - \frac{\Sigma H}{D_\pm^2 - m^2}\Big)\Big)^{-1}$$

$$\approx G^{R(A)}\gamma_0\Big(1 + \frac{\Sigma H}{D_\pm^2 - m^2} + \frac{\frac{1}{4}H^2}{(D_\pm^2 - m^2)^2}\Big), \tag{21}$$

where $D_\pm^\mu = \partial^\mu - ie\mathcal{A}_H^\mu \pm \delta^{\mu 0}\epsilon$.

Magnetoconductivity and chiral density from NDT

$$j^{\mu} = \mathrm{tr}\ \gamma^0 \gamma^{\mu} i G_1^{<}(x,x) \sim \quad \gamma^{\mu}$$

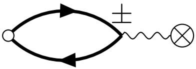

$$E_j \quad , \qquad (22)$$

the same for $\rho_5 = \mathrm{tr}\ \gamma_5 i G_1^{<}(x,x)$.

Magnetoconductivity and chiral density from NDT

$$j^\mu = \mathrm{tr}\ \gamma^0 \gamma^\mu i G_1^<(x,x) \sim \quad \gamma^\mu$$

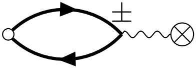

$$E_j \quad , \qquad (22)$$

the same for $\rho_5 = \mathrm{tr}\ \gamma_5 i G_1^<(x,x)$.

$$G^{1-+}_{p+q,p} =$$

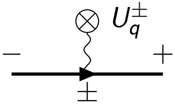

$$= G^{--}_{p+q} U_q^- G_p^{-+} + G^{-+}_{p+q} U_q^+ G_p^{++}.$$

Magnetoconductivity and chiral density from NDT

$$j^{\mu} = \mathrm{tr}\, \gamma^0 \gamma^{\mu} i G_1^{<}(x,x) \sim \quad \gamma^{\mu}$$

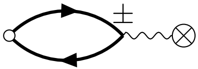

$$E_j \quad , \tag{22}$$

the same for $\rho_5 = \mathrm{tr}\, \gamma_5 i G_1^{<}(x,x)$.

$$G^{1-+}_{p+q,p} =$$

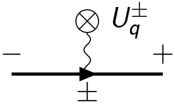

$$= G^{--}_{p+q} U^{-}_{q} G^{-+}_{p} + G^{-+}_{p+q} U^{+}_{q} G^{++}_{p} .$$

$$U^{\pm}_{q} = \pm \gamma_0 \gamma_j \mathcal{A}^j(q), \quad \mathcal{A}^j(q) = -iE^j (2\pi)^4 \delta(\mathrm{q}) \delta'(q_0), \tag{23}$$

Magnetoconductivity and chiral density from NDT

$$j^\mu = \mathrm{tr}\ \gamma^0\gamma^\mu iG_1^<(x,x) \sim \quad \gamma^\mu$$ 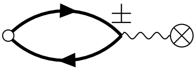

$$E_j \quad , \qquad (22)$$

the same for $\rho_5 = \mathrm{tr}\ \gamma_5 iG_1^<(x,x)$.

$$G^{1-+}_{p+q,p} =$$ 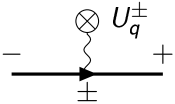

$$= G^{--}_{p+q}U_q^- G_p^{-+} + G^{-+}_{p+q}U_q^+ G_p^{++}.$$

$$U_q^\pm = \pm\gamma_0\gamma_j\mathcal{A}^j(q), \quad \mathcal{A}^j(q) = -iE^j(2\pi)^4\delta(\mathrm{q})\delta'(q_0), \qquad (23)$$

$$G^<_{1p} = -2iE^j\,\mathrm{Re}(\partial_0 G_p^<\alpha_j G_p^A) \qquad (24)$$

Magnetoconductivity and chiral density from NDT

With the Pauli-Villars regularization

$$\rho_5 = 2\,\mathrm{Re}\int_p^{(R)} \mathrm{tr}\;\gamma_5 E^j \partial_0 G_H^< \alpha_j G_H^A \tag{25}$$

(27)

Magnetoconductivity and chiral density from NDT

With the Pauli-Villars regularization

$$\rho_5 = 2\,\mathrm{Re}\int_p^{(R)} \mathrm{tr}\ \gamma_5 E^j \partial_0 G_H^< \alpha_j G_H^A \tag{25}$$

$$\ldots \approx \frac{E^j H_j}{4\pi^2\epsilon}\int_0^{+\infty} P^2 dP\left(\frac{\Theta(\mu - E)}{E^3} + \frac{1}{E^3} - \frac{1}{E_R^3}\right) \tag{26}$$

(27)

Magnetoconductivity and chiral density from NDT

With the Pauli-Villars regularization

$$\rho_5 = 2\,\mathrm{Re}\int_p^{(R)} \mathrm{tr}\ \gamma_5 E^j \partial_0 G_H^< \alpha_j G_H^A \qquad (25)$$

$$\ldots \approx \frac{E^j H_j}{4\pi^2\epsilon}\int_0^{+\infty} P^2 dP\Big(\frac{\Theta(\mu - E)}{E^3} + \frac{1}{E^3} - \frac{1}{E_R^3}\Big) \qquad (26)$$

$$\approx \frac{E^j H_j}{4\pi^2}\ \frac{1}{2\epsilon}\ln\left(4\frac{\mu^2}{m^2}\right), \quad \mu^2 \gg m^2. \qquad (27)$$

Magnetoconductivity and chiral density from NDT

With the Pauli-Villars regularization

$$\rho_5 = 2\,\mathrm{Re}\int_p^{(R)} \mathrm{tr}\ \gamma_5 E^j \partial_0 G_H^< \alpha_j G_H^A \tag{25}$$

$$\ldots \approx \frac{E^j H_j}{4\pi^2\epsilon}\int_0^{+\infty} P^2 dP\Big(\frac{\Theta(\mu - E)}{E^3} + \frac{1}{E^3} - \frac{1}{E_R^3}\Big) \tag{26}$$

$$\approx \frac{E^j H_j}{4\pi^2}\ \frac{1}{2\epsilon}\ln\left(4\frac{\mu^2}{m^2}\right), \quad \mu^2 \gg m^2. \tag{27}$$

$$\sigma_{jk} = 2\,\mathrm{Re}\int_p^{(R)} \mathrm{tr}\ \alpha_k \partial_0 G_H^< \alpha_j G_H^A \ \rightarrow\ \sigma_{jk}^{(1)} = 0,\ \sigma_{jk}^{(2)}. \tag{28}$$

Magnetoconductivity and chiral density from NDT

With the Pauli-Villars regularization

$$\rho_5 = 2\,\mathrm{Re}\int_p^{(R)} \mathrm{tr}\;\gamma_5 E^j \partial_0 G_H^< \alpha_j G_H^A \tag{25}$$

$$\ldots \approx \frac{E^j H_j}{4\pi^2 \epsilon}\int_0^{+\infty} P^2 dP\left(\frac{\Theta(\mu - E)}{E^3} + \frac{1}{E^3} - \frac{1}{E_R^3}\right) \tag{26}$$

$$\approx \frac{E^j H_j}{4\pi^2}\,\frac{1}{2\epsilon}\ln\left(4\frac{\mu^2}{m^2}\right), \quad \mu^2 \gg m^2. \tag{27}$$

$$\sigma_{jk} = 2\,\mathrm{Re}\int_p^{(R)} \mathrm{tr}\;\alpha_k \partial_0 G_H^< \alpha_j G_H^A \;\to\; \sigma_{jk}^{(1)} = 0,\; \sigma_{jk}^{(2)}. \tag{28}$$

$$\sigma_{jk}^{(2)} \approx \frac{3}{2}\,\frac{H_j H_k}{4\pi^2}\,\frac{1}{\epsilon^2}\,\frac{1}{2\epsilon}\ln\left(\frac{4\mu^2}{m^2}\right) \tag{29}$$

Magnetoconductivity and chiral density from NDT

In the limit $\mu^2 \gg m^2$, $\frac{u\mu}{T} \ll 1$ with the dissipation rate ϵ substituted

$$\rho_5 \approx \frac{E^j H_j}{4\pi^2} \, \frac{2\pi\rho_0 u^2}{w^2\mu^2 T} \, \frac{1}{2} \ln\left(4\frac{\mu^2}{m^2}\right), \tag{30}$$

$$\sigma^{(2)}_{jk} \approx \frac{3}{2} \, \frac{H_j H_k}{4\pi^2} \left(\frac{2\pi\rho_0 u^2}{w^2\mu^2 T}\right)^3 \frac{1}{2} \ln\left(\frac{4\mu^2}{m^2}\right) \tag{31}$$

Results summary

CKT & CME	our NDT calculation

Results summary

CKT & CME	our NDT calculation
$\rho_5 = \frac{E^j H_j}{4\pi^2}\ \tau_5$	$\rho_5 \approx \frac{E^j H_j}{4\pi^2}\ \frac{1}{2\epsilon} \ln\left(4\frac{\mu^2}{m^2}\right)$

Results summary

CKT & CME	our NDT calculation
$\rho_5 = \frac{E^j H_j}{4\pi^2}\ \tau_5$	$\rho_5 \approx \frac{E^j H_j}{4\pi^2}\ \frac{1}{2\epsilon} \ln\left(4\frac{\mu^2}{m^2}\right)$
$\sigma_{ij}^{CME} = \frac{3}{2}\ \frac{H_i H_j}{4\pi^2}\ \frac{v_F^3}{\pi^2 T^2 + \mu^2}\ \tau_5$	$\sigma_{jk}^{(2)} \approx \frac{3}{2}\ \frac{H_j H_k}{4\pi^2}\ \frac{1}{\epsilon^2}\ \frac{1}{2\epsilon} \ln\left(\frac{4\mu^2}{m^2}\right)$
	where $\epsilon \approx \frac{1}{2\pi}\frac{w^2}{\rho_0}\frac{\mu^2 T}{u^2}$,
	at $m^2 \ll \mu^2$ and $\frac{u\mu}{T} \ll 1$

Results summary

CKT & CME	our NDT calculation
$\rho_5 = \frac{E^j H_j}{4\pi^2}\ \tau_5$	$\rho_5 \approx \frac{E^j H_j}{4\pi^2}\ \frac{1}{2\epsilon} \ln\left(4\frac{\mu^2}{m^2}\right)$
$\sigma_{ij}^{CME} = \frac{3}{2}\ \frac{H_i H_j}{4\pi^2}\ \frac{v_F^3}{\pi^2 T^2 + \mu^2}\ \tau_5$	$\sigma_{jk}^{(2)} \approx \frac{3}{2}\ \frac{H_j H_k}{4\pi^2}\ \frac{1}{\epsilon^2}\ \frac{1}{2\epsilon} \ln\left(\frac{4\mu^2}{m^2}\right)$
	where $\epsilon \approx \frac{1}{2\pi} \frac{w^2}{\rho_0} \frac{\mu^2 T}{u^2}$,
	at $m^2 \ll \mu^2$ and $\frac{u\mu}{T} \ll 1$

$$\tau_5 \sim \frac{1}{2\epsilon} \ln\left(\frac{4\mu^2}{m^2}\right) \sim \frac{\pi \rho_0 u^2}{w^2 \mu^2 T} \ln\left(\frac{4\mu^2}{m^2}\right) \tag{32}$$

Backup Slides. Strong magnetic field limit

At $2eH > \mu^2 \gg m^2$

$$\hat{G}_{p_0 p_2 p_3}(x_1, x_2) \approx \hat{G}^{(\mathrm{LLL})}_{p_0 p_2 p_3}(x_1, x_2) = \tag{33}$$

Backup Slides. Strong magnetic field limit

At $2eH > \mu^2 \gg m^2$

$$\hat{G}_{p_0 p_2 p_3}(x_1, x_2) \approx \hat{G}^{(\mathrm{LLL})}_{p_0 p_2 p_3}(x_1, x_2) =$$

$$= \hat{\hat{G}}_{p_0 p_3} O^- \sqrt{\frac{H}{\pi}} e^{-\frac{H}{2}((x_1 - \frac{p_2}{H})^2 + (x_2 - \frac{p_2}{H})^2)}, \qquad (33)$$

Backup Slides. Strong magnetic field limit

At $2eH > \mu^2 \gg m^2$

$$\hat{G}_{p_0 p_2 p_3}(x_1, x_2) \approx \hat{G}^{(\mathrm{LLL})}_{p_0 p_2 p_3}(x_1, x_2) = \\ = \hat{\hat{G}}_{p_0 p_3} O^- \sqrt{\frac{H}{\pi}} e^{-\frac{H}{2}((x_1 - \frac{p_2}{H})^2 + (x_2 - \frac{p_2}{H})^2)}, \tag{33}$$

where

$$O^- = \frac{1}{2}(1 + i\gamma_1\gamma_2 \,\mathrm{sign}(eH_3)) \tag{34}$$

is a projector.

Backup Slides. Strong magnetic field limit

At $2eH > \mu^2 \gg m^2$

$$\hat{G}_{p_0 p_2 p_3}(x_1, x_2) \approx \hat{G}^{(\mathrm{LLL})}_{p_0 p_2 p_3}(x_1, x_2) =$$
$$= \hat{\tilde{G}}_{p_0 p_3} O^- \sqrt{\frac{H}{\pi}} e^{-\frac{H}{2}((x_1 - \frac{p_2}{H})^2 + (x_2 - \frac{p_2}{H})^2)}, \tag{33}$$

where

$$O^- = \frac{1}{2}(1 + i\gamma_1\gamma_2 \,\mathrm{sign}(eH_3)) \tag{34}$$

is a projector.
The reduced 2D Keldysh-Green functions are

$$\tilde{G}^{R(A)} = (p_0 \pm i\epsilon_H - \alpha_3 p_3 - \gamma_0 m)^{-1}, \tag{35}$$

$$\tilde{G}^{<} = (\tilde{G}^A - \tilde{G}^R) n(p_0), \quad \tilde{E} = \sqrt{p_3^2 + m^2} \tag{36}$$

Backup Slides. Strong magnetic field limit

Than the result reads

$$\rho_5 = \frac{E_j H^j}{2\pi^2} \frac{1}{2\epsilon_H} \ln\left(4\frac{\mu^2}{m^2}\right), \tag{37}$$

$$\sigma_{kj} = \frac{H_j H_k}{2\pi^2 |\vec{H}|} \frac{1}{2\epsilon_H} \ln\left(4\frac{\mu^2}{m^2}\right), \quad 2eH > \mu^2 \gg m^2, \tag{38}$$

Backup Slides. Strong magnetic field limit

Than the result reads

$$\rho_5 = \frac{E_j H^j}{2\pi^2} \frac{1}{2\epsilon_H} \ln\left(4\frac{\mu^2}{m^2}\right), \tag{37}$$

$$\sigma_{kj} = \frac{H_j H_k}{2\pi^2 |\vec{H}|} \frac{1}{2\epsilon_H} \ln\left(4\frac{\mu^2}{m^2}\right), \quad 2eH > \mu^2 \gg m^2, \tag{38}$$

where to fix the dissipation rate expression, the density of states at the Fermi sphere surface is to be replaced with the density of state at the Landau level, $\mu^2 \to |H|$

$$\epsilon_H \approx \frac{w^2}{\rho_0} \frac{T}{u^2} \frac{|H|}{4\sqrt{2}}. \tag{39}$$